Design and dynamic investigation of low-grade power generation systems with CO_2 transcritical power cycles and R245fa organic Rankine cycles

L. Li[a], Y.T. Ge[b*], X. Luo[c], S.A. Tassou[d]

[a]School of Engineering and Technology, University of Hertfordshire, Hatfield, Hertfordshire, AL10 9AB, UK

[b]Sustainable Environment Research Centre, Faculty of Computing, Engineering and Science, University of South Wales, Pontypridd, CF37 1DL, UK

[c]National Key Laboratory of Science and Technology on Aero Engines Aero-thermodynamics, The Collaborative Innovation Centre for Advanced Aero-Engine of China, Beihang University, Beijing 10191, China

[d]RCUK National Centre for Sustainable Energy Use in Food Chains (CSEF), Institute of Energy Future, Brunel University London, Uxbridge, Middlesex, UB8 3PH, UK

ABSTRACT

This paper deals with the dynamic experimental investigation on low-grade power generation systems with CO_2 transcritical power cycles (T-CO_2) and R245fa organic Rankine cycles (ORC). These two systems were heated indirectly by exhaust gases of an 80 kWe micro-turbine CHP unit through a hot thermal oil system. The main components of each test system included a plate-type gas generator/ evaporator, a turboexpander with high speed generator, a finned-tube air cooled condenser and a liquid pump. Both test rigs were fully commissioned and instrumented from which comprehensive dynamic experimental investigations were conducted to examine the effects of some important dynamic operational processes on system performance. These included the system start-up, variation of working fluid pump speed, change of thermal oil pump speed and system shutdown. These can lead to fully understand the dynamic and inertia behaviours of the system operations and thus to obtain robust controls. The experimental results reveal that working fluid mass flow rates are affected significantly by the start-up and shutdown processes, followed by the temperatures and

pressures at turbine inlets and outlets. The research outcomes can contribute significantly to understand the system dynamic operating processes and thus instruct the system controls and safety operations.

Keywords: CO_2 transcritical power cycle, R245fa organic Rankine cycle, dynamic investigation, experimental transient performance.

Corresponding author. Tel.: +44 1443 482165

Email address: Yunting.Ge@southwales.ac.uk (Y.T. Ge).

Nomenclature

h	enthalpy (J/kg)
$\dot{m}$	mass flow rate (kg/s)
W	power generation (W)

Greek symbols

η	efficiency

Subscripts

all	overall
f	working fluid
is	isentropic
m	measured
t	turbine
1	turbine inlet
2	turbine outlet

1. Introduction

The consumption of fossil fuels in power generation is continuously increasing which has been leading to more serious environmental issues such as excessive CO_2 emissions, severe atmospheric pollution and high energy cost etc. Subsequently, there is an urgent obligation to generate power using industrial waste heat [1] and renewable energy [2] with low temperatures typically ranging from 100 °C to 350 °C and applicable thermodynamic power cycles such as Organic Rankine Cycle (ORC) [3] , transcritical power cycle (TPC) [4], trilateral flash cycle [5] and Brayton cycle [6] etc. Among these technologies, ORC and TPC promise high potential and therefore are widely applied in industrial applications and small-scale energy productions.

Compared to a century-old steam Rankine power plant, the ORC system has the similar working mechanism for power generation but uses an organic working fluid instead such as R245fa, which has a lower boiling point at higher pressure and is condensable at lower pressure. Thus, the ORC system is expected to achieve a higher efficiency with greater power generation when applied to a low-grate heat source [7]. However, a common challenge for any ORC system is the optimal selection of appropriate working fluid and particular design of thermodynamic power cycle. By the theoretical study on nine applicable working fluids for ORC, R245fa was found to be the most suitable one for an engine waste heat-recovery application when safety levels were inclusively consisted [8]. In another research, a zeotropic fluid of R152a/R245fa with different compositions were applied and compared in low-grade ORC systems [9]. It was demonstrated that pure R245fa of the mixture could present the highest thermal efficiency but required larger expander size and consequent higher system cost. Further balance and compromise need to be considered when selecting an ORC working fluid. On the other hand, from the environmental impact point of view, the conventional ORC working fluid HFCs have zero Ozone Depletion Potential (ODP) but mostly have higher Global Warming Potentials (GWP). Such evidences will definitely affect long-term utilisation of HFC working fluids in ORCs. Subsequently, some natural working fluids such as CO_2 and NH_3 tend to be more attractive in the applications of low-grade power generation systems [10].

As listed in Table 1, CO_2 is an environmental friendly natural working fluid with no safety matter. In addition, CO_2 has superb thermophysical properties, despite its high critical pressure and low critical temperature, and lower manufacturing cost than the organic fluids since it can be obtained from waste products of many industry processes. Nevertheless, the feasibility of CO2 working fluid in low-grade power generation needs to be investigated. Correspondingly, a thermodynamic analysis and comparison between CO_2 transcritical power cycle (T-CO_2) and R245fa organic Rankine cycle have been researched [11]. The research results revealed that the thermal and exergy efficiencies of the T-CO_2 system were slightly lower than those of R245fa ORC system. In addition, the energetic and exergetic analyses and comparisons of transcritical power cycles with both CO_2 and R32 working fluids were investigated [12]. The results showed that R32 system could achieve higher thermal efficiency but operated at much lower pressures. For a T-CO_2 system, CO_2 is most likely operating at higher pressure of about 120 bar or above such that the system components and controls need to be specially designed. One feasible way to utilise CO_2 as a working fluid and maintain relatively low operating pressure is to mix CO_2 with one of ORC fluids such as R161and R152a [13] or isopentane and propane [14].

Although a large body of theoretical research has been conducted on the ORC and T-CO_2 systems, experimental investigations on these systems are even more important to valid the theoretical analyses and verify system design and operation. Moreover, during the theoretical investigations, the efficiencies and power generations of the system turbine or expansion machine are usually kept constants when different working fluids are employed which however are difficult to be controlled and maintained in experimental operations unless the systems are in steady states. A domestic-scale R245fa ORC system with a hermetic scroll expander has been researched experimentally [15] in which a global electric efficiency was around 8% at steady state when the expander inlet temperatures were in a range of 120-150°C. In another research, a single-stage axial flow turbine was utilised in a regenerative R245fa ORC system in which the maximum steady power outlet and system efficiency could reach 6 kW and 7.98% respectively at heat source temperature about 130°C[16]. For the T-CO_2 systems, a number of relevant researches can be found from literatures. Typically, CO_2 transcritical power cycles driven by solar energy were constructed and investigated experimentally at steady states with the system power generation efficiency between 8.78 % and 9.45% [17, 18].

Although a number of experimental investigations on both ORC and T-CO_2 systems have been carried out, most of the research outcomes were based on steady states . Practically, either ORC or T-CO2 systems operate under transient or quasi- transient conditions such as the waste heat recoveries from automotive and biomass boilers. The dynamic process analyses of heat source and working fluid pump could lead to optimal system controls so that the system can utilise efficiently the applicable heat source thus achieve better and safety performances [19]. From the literature reviews, a zeotropic mixture of R245fa and R365mfc was studied by focusing on its dynamic behaviours in the ORC system and the performance in each system component [20]. In addition, a kW-scale R123 ORC system with a turbine to examine the heat transfer and dynamic power conversion processes was constructed and tested [21]. The experimental results indicated that the mass flow rate through the turbine was different from that through the pump during the dynamic test. Therefore, the comprehensive dynamic experimental analysis for ORC and T-CO_2 systems during different operating processes need to be further investigated and developed. Move over , in order to further optimise the T-CO_2 and R245fa ORC control systems, the start-up and shutdown processes of both systems need to be conducted, which have not been investigated so far.

Subsequently, in this study, an experimental investigation was conducted on small-scale T-CO2 and R245fa ORC system test rigs coupled to an 80 kWe CHP unit with hot thermal oil system. The CO_2 and R245fa turbines were employed to convert thermal energy into electricity in each system. Dynamic behaviours of both systems are demonstrated with time during various important operational processes. These include both system start-up processes, response of R245fa ORC system against variation of working fluid pump conditions, responses of T-CO_2 system against variation of thermal oil pump condition and both system shutdown processes. The investigated results have significant contributions to the component and control designs for both systems.

2. Experimental facility and methodology

Fig. 1 shows the schematic diagram of the CHP, T-CO_2 and ORC systems, which have been set up in the laboratory at Brunel University London. Each of the T-CO_2 and ORC systems was classified into two group levels with different colours in which red indicates the high temperature level while blue the low temperature level. In addition, each system consisted of four separate fluid loops, i.e., the exhaust gas, thermal oil, CO_2/ R245fa, and ambient air. The heat source for both the T-CO_2 and ORC systems was the exhaust flue gases from an 80 kWe CHP unit. The high temperature exhaust flue gases passed through an integrated thermal oil boiler of the CHP and heated the thermal oil through the intermediate thermal oil loop . The high temperature thermal oil was then circulated by a variable speed oil pump through a plate-type heat exchanger which was acted as either CO_2 gas generator or ORC evaporator. The CO_2 or R245fa ORC fluid was then heated up or evaporated and superheated before being expanded in each expander.

Accordingly, the T-CO_2 or R245fa ORC system was mainly comprised of a thermal oil-heated gas generator or a evaporator, a turbo expander with high speed generator, a finned-tube air-cooled condenser and a working fluid liquid pump, as shown in Fig1 and Fig.2 (photos). The high pressure CO_2 or R245fa flow was heated through the gas generator or evaporator and left as a high temperature or superheated vapour. The vapour working fluid (CO_2 or R245fa) with high pressure and higher temperature was then expanded through the CO_2 or R245fa turbine, as shown in Fig.3. The expansion process in the CO_2 or R245fa turbine turned a shaft and its magnetic coupling connection to drive a permanent magnet synchronous generator at a rated rotation speed of up to 18,000 rpm. Each generator delivered electric power to the campus electric grid by means of a smart inverter and transformer. The ABB smart inverter in each turbine system allowed the generator speed to be matched and monitored with the electric power generated so that each turbine and generator could operate smoothly. In order to create bypass for the CO_2 and R245fa flow whenever necessary, two throttle valves were installed separately in parallel to the CO_2 and R245fa turbines, as shown in Fig. 1.

After expansion (Point 2), the low pressure CO_2 or R245fa vapour was extracted from each individual turbine and flew to one assigned finned-tube air cooled condenser, which used ambient air to condense the CO_2 or R245fa fluid from a superheated into liquid state at Point 4. The ambient air flow rate through each condenser was controlled using a variable speed fan installed above the condenser. In addition, the ambient air temperature was adjusted by mixing warm exhaust air from the condenser and cold inlet ambient air through four recircular fans installed on each corner side of the condenser outlet, as shown in Fig. 2. Each condenser outlet was connected by a liquid receiver to ensure no vapour cavitation at each working fluid pump inlet. The liquid level in each liquid receiver was also monitored by a fitted sight glass to indicate if there was sufficient liquid stored. A triplex plunger CO_2 pump fed the low pressure liquid CO_2 from Point 5 into the high pressure gas generator at Point 6 while a seal-less diaphragm type R245fa pump circulated the low pressure R245fa liquid from Point 5 into high pressure evaporator at Point 6. Thereafter, the T-CO_2 or ORC cycle repeated in each closed loops. The running speed of the liquid CO_2 or R245fa pump was also adjusted by a frequency drive inverter, as shown in Fig. 2, which could control the CO_2 or R245fa working fluid mass flow rate and operating pressure in each system.

Temperature sensors and pressure transducers were placed at the inlet and outlet of each main system component and a number of fluid mass flow meters were also installed in each system, as shown in Fig.1. Table 2 shows the measurement principle, measuring range and accuracy of these measurement devices. The hot thermal oil temperatures were measured with inflow K-type thermocouples with accuracy of ±0.5°C at prior and after the gas generator or evaporator. For the T-CO_2 system, the temperatures were measured by inline K-type thermocouples with ±0.5°C accuracy while the pressures were measured with MBS 33 pressure transducers of ±0.3% accuracy and 0.5s response time. A twin V-shaped tube type mass flow meter with 0-1800 kg/h range and ±0.1% accuracy was used to measure the liquid CO_2 mass flow rate. For the R245fa ORC system, the temperatures were measured with inflow K-type thermocouples of ±0.5°C accuracy to get the most precise temperature reading while the pressures were measured using AKS 32 pressure transducers with ±0.3% accuracy and 0.5s response time. The liquid R245fa mass flow rate was measured by a twin tube type mass flowmeter with 0-6500kg/h range and ±0.15% accuracy. In addition, a power meter with accuracy of ±0.8% was used to determine the output current, voltage and power of CO_2 turbine or R245fa turbine of each system. Each system condenser had a hot wire anemometer with an accuracy class of ±0.15 m/s at full range of 1.27-78.7 m/s to measure the ambient air velocity and two K-type thermocouples at the inlet and outlet of each condenser. The data acquisition unit for the T-CO_2 or ORC system was from CompaqDAQ (National Instruments data logger system) connected with LabVIEW software to record and present the measurements from thermocouples, pressure sensors and mass flow meters.

3. Results and analysis

The method to evaluate transient performances of the T-CO_2 and ORC systems at different operating conditions is proposed in this paper. It consists of four parts: analysis of each system start-up process and preliminary test, response of the R245fa ORC system performance against different working fluid pump speeds, response of the T-CO_2 system against different thermal oil pump speeds and analysis of each system shutdown process. During the tests, the CO_2 and R245fa pump frequencies were controlled to be changed from 0Hz to 35 Hz and 0 Hz to 40 Hz respectively, while the thermal oil pump frequencies were controlled to be varied from 0 Hz to 25 Hz and 0 Hz to 50 Hz for the T-CO_2 and R245fa ORC systems individually. These setting were designed to ensure that the inlet working fluid temperature was below maximum value at 110 °C (120 °C for a short operational period) for each turbine and the working fluid inlet pressure was below 110 bar for the CO_2 turbine and less than 14 bar for the R245fa turbine as required by the turbine manufacturers. In addition, all the thermophysical properties of CO_2 and R245fa such as entropy and enthalpy etc. were calculated using REFPROP 8.0 software [22] based on the temperature and pressure measured at each point.

3.1 Analysis of the system start-up processes and preliminary tests

Purposely, transient processes of the T-CO_2 and R245fa ORC test systems operated and were recorded separately from the system start up to steady state and then working fluid mass flow rate increased abruptly to steady condition again. For the T-CO_2 system, the dynamic process took about 52 min while the R245fa ORC continued roughly 120 min to complete ,in which, for the system start-up processes, the T-CO_2 and ORC systems took around 19 min and 40 min respectively. It is noticed that the start-up process of T-CO_2 system was much faster than that of the R245fa ORC system.

The dynamic variations of cycle point temperatures at the inlet and outlet of each turbine and working fluid mass flow rate of each system are plotted and demonstrated in Fig.4. For each cycle, when the system started up, the working fluid mass flow rate increased immediately to a peak value and then dropped abruptly to reach steady state. After that, the motor frequency of each system liquid pump was controlled to step up such that the working fluid mass flow rate amplified instantly and thereafter reached another steady state. Correspondingly, for each system, with the system start up, the turbine inlet and outlet temperatures both increased and decreased a bit once the working fluid mass flow rate dropped from its peak value. These two working fluid temperatures then approached gradually to their steady states and thereafter dropped abruptly with the sudden went up of working fluid mass flow rate and then quickly reached to their steady states.

At the same time period shown in Fig. 4, the dynamic variations of working fluid pressures at the inlet and outlet of each turbine were recorded and depicted in Fig.5. In the start-up process, for each system the turbine inlet and outlet pressures both increased immediately when the working fluid pump started up. The high pressure working fluid flowed rapidly into the turbine, passed through the turbine blades and reduced the working fluid pressure at the turbine outlet. Thereafter two working fluid pressures reached moderately to their steady state. As expected, when further increased working fluid mass flow rate of each system, the working fluid pressures at turbine inlet and outlet both increased immediately with higher working fluid mass flow rate and then came to their steady states again.

At the same time periods, the dynamic variations of turbine power generation and pressure ratio of each turbine are plotted in Fig. 6. The pressure ratio of turbine was calculated by the pressures at the turbine inlet and outlet while the actual turbine power output was measured directly by a power meter installed at outlet wire of each turbine. In the start-up process, for each system, the turbine output and pressures ratio both increased immediately to the peak values and then dropped to troughs. After that, the turbine power output and pressure ratio increased gradually to their steady states. The troughs for turbine power output and pressure ratio were caused by the sudden changes of the temperature and pressure differences and working fluid mass flow rates. As the working fluid mass flow rate suddenly increased, the turbine power output and pressure ratio both augmented significantly and reached steady states again for the T-CO_2 system. However, for the R245fa ORC system, the variation trends of the turbine power outlet and pressure ratio were relatively small due to the lower turbine inlet and outlet pressure increases. Consequently, the turbine power outlet could reach around 494 W and 655 W in the dynamic processes for the T-CO_2 and R245fa ORC systems respectively.

Meanwhile, the dynamic variations of working fluid temperatures at the inlet and outlet of each condenser were recorded and are plotted in Fig. 7. For each system, the start-up process and preliminary test affected significantly on each condenser inlet temperature rather than on the condenser outlet. The variation tendency of condenser inlet temperature was more or less the same as the corresponding turbine outlet temperature considering only the connection pipe and fitting temperature losees involved. Meanwhile, the condenser outlet temperature of each system varied a little during the start-up process and preliminary test period considering of constant heat sink parameters and higher condenser performance.

3.2 Response of R245fa ORC system against variation of working fluid pump condition

As shown in Fig. 1, a R245fa liquid pump was installed after the liquid receiver in the R245fa ORC system. In addition, a frequency drive inverter was attached to the R245fa liquid pump. Therefore, the R245fa liquid pump speed could be controlled by the modulation of ORC pump frequency. To investigate the dynamic processes of R245fa ORC system against variable working fluid pump speeds, a test matrix of working fluid pump speed swing was designed and is listed in Table 3. For each stage of the test, only the condition of working fluid pump speed was adjusted, while the parameters of heat source (thermal oil) and sink (ambient air) remained unvaried. In the first stage of the test, a lower ORC pump converter frequency of 37.5 Hz was maintained until the ORC system approached to steady state. After 30 min, ORC pump condition was quickly switched to higher frequency of 40 Hz unit and the ORC system turned to steady state again. After 35 min, the ORC pump condition was quickly switched back to a further lower ORC pump converter frequency of 35 Hz and maintained for 30 min to steady condition again.

Correspondingly, the dynamic variations of ORC pump speed and R245fa mass flow rate were therefore recorded and are plotted in Fig. 8. The ORC pump speed increased with a higher converter frequency and decreased with a lower frequency but not in a monotonically adjusting manner. The peak and lowest values were formed on the ORC pump speed curve. In addition, it can be seen that the mass flow rate could sensitively follow the change of the ORC pump speed, which was changed by the pumping frequency, without apparent time delay. From stage I to stage II, R245fa mass flow rate increased by 3.26%, which naturally brought a significant increase of ORC pump speed from 730 RPM to 779 RPM. Furthermore, from stage II to stage III, R245fa mass flow rate decreased by 9.8%, which in turn led to a larger decrease of ORC pump speed from 779 RPM to 680 RPM.

At the same time period , the dynamic variations of working fluid temperatures and pressures at the inlet and outlet of the R245fa turbine were measured and are shown in Fig. 9. The R245fa turbine inlet and outlet temperatures were dropped down as soon as the R245fa ORC pump was switched to a higher speed except that the turbine outlet temperature decreased in a larger extent than the turbine inlet temperature, which indicates that the temperature at low pressure side (turbine outlet) is more sensitive than that of high pressure side (turbine inlet)to the pump speed. However, when the R245fa ORC pump was switched back to a lower speed, the temperature at the turbine inlet and outlet fluctuated slightly and increased in a manner similar to the system start-up process. In percentage, when the ORC pump speed increased from 730 RPM to 779 RPM, the R245fa turbine inlet and outlet temperatures decreased by 0.97% and 7.3% respectively. On the other hand, when the R245fa ORC pump speed decreased from 779 RPM to 680 RPM, the cycle point temperatures of turbine inlet and outlet amplified 11.54% and 23.88% respectively. However, the pressures of turbine inlet and outlet had the similar variation tendency with ORC pump speed and R245fa mass flow rate during this period. Unlike other parameters, the pressures of turbine inlet and outlet went through little variation with 1.54% and 2.15% when the ORC pump speed increased from 730 RPM to 779 RPM, 4.79% and 7% when the ORC pump speed decreased from 779 RPM to 680 RPM respectively.

Meanwhile, the dynamic variations of the ORC working fluid temperatures and pressures at condenser inlet and outlet were recorded and are shown in Fig. 10. The condenser inlet temperature and pressure fluctuated slightly during each stage and changed in a manner similar to the turbine outlet temperature and pressure when the ORC pump speed changed.

However, the condenser inlet temperature and pressure was lower than those at the turbine outlet by about 1.98°C and 0.84 bar respectively at each stage. In addition, this result also shows that the condenser outlet temperature and pressure could be almost immune to the variation of ORC pump conditions, which ensured the continuous operation of ORC system.

Table 3 shows the summarised working condition in this transient test. For each steady state condition, the turbine overall efficiency is calculated with equation 1.

$$\eta_{t,all} = \frac{W_{t,m}}{\dot{m}_f(h_1 - h_{2,is})} \tag{1}$$

Thus, during this transient test (from stage I to stage III), the measured turbine power generations were 694.44 W, 697.12 W and 686.52 W respectively. Correspondingly, the calculated turbine overall efficiency were 15.7%, 16.0% and 15.3% each .

3.3 Response of T-CO_2 system against variation of thermal oil pump condition

To examine the effect of the heat source mass flow rate on the T-CO_2 system performance, the thermal oil flow rate was controlled to vary from 0.46 kg/s to 0.36 kg/s by modulating the oil pump frequency from 25 Hz to 20 Hz. The inertia behaviour when thermal oil brought the thermal energy from the exhaust gas to the T-CO_2 system could be helpful against the variation of exhaust gas temperature. Thus, when the oil pump frequency changed from 25 Hz to 20 Hz, the thermal oil temperature was varied automatically from 139.6°C to 144.1°C without modulating the CHP power outlets. In the meantime, as listed in Table 4, all parameters of T-CO_2 system such as CO_2 pump frequency, condenser air velocity and ambient air temperature were remain unvaried due to its larger inertia.

Subsequently, the dynamic variations of the thermal oil inlet and outlet temperatures were measured and are shown in Fig. 11. In the first stage of the test, higher thermal oil mass flow rate of 0.46 kg/s and 139.6°C thermal oil temperature were maintained until T-CO_2 system was at steady state. Then thermal oil mass flow rate was quickly switched by hand to 0.36 kg/s and maintained to steady state again. During this process, the thermal oil temperature approached gradually to their steady state at 144.1°C.However, the thermal oil outlet temperature wend down as soon as the thermal oil pump was switched to lower frequency and thereafter increased moderately to steady state again. In percentage, the thermal oil inlet temperature increased by 3.25% and thermal oil outlet temperature decreased by 8.9% when the thermal oil mas flow rate reduced from 0.46 kg/s to 0.36 kg/s.

Correspondingly, the dynamic variations of working fluid temperatures and pressures at CO_2 turbine inlet and outlet are shown in Fig. 12. The CO_2 turbine inlet and outlet temperatures were decreased at larger extents than the changes of thermal oil outlet temperatures when the thermal oil mass flow rate was changed to a lower value, as shown in Fig. 10, which means that the inertia and thermal capacity of thermal oil cycle are much bigger than that of T-CO_2 system. In addition, when the thermal oil mass flow rate reduced, the variations of CO_2 turbine inlet pressures had the similar tendency with those of CO_2 turbine temperatures. However, the turbine outlet pressure was almost kept steady state when the thermal oil mass flow rate decreased. Not many random pressure values were observed in the results due to high accuracy of pressure transducers and smooth flow through the CO_2 turbine. Quantitatively, when the thermal oil mass flow rate decreased from 0.46 kg/s to 0.36 kg/s, the percentage decrease rates of turbine inlet temperature, turbine outlet temperature, turbine inlet pressure and turbine outlet pressure were 11.03%, 12.72% , 2% and 0.6% respectively.

Meanwhile, the dynamic variations of temperatures and pressures at the CO_2 condenser inlet and outlet are depicted in Fig. 13. As expected, the condenser inlet temperature and pressure had the similar variation tendency with the turbine outlet temperature and pressure when the thermal oil mass flow rate reduced. However, condenser outlet temperature pattern matched the ambient air trend and the CO_2 was cooled down to approximately 26°C during the steady state and dynamic processes. As predicted, the condenser outlet pressure had the same pattern as the condenser inlet pressure and the steady state pressure was around 66 bar, implying that the CO_2 pressure loss is negligible during the condensation process, which is different from the larger condenser pressure loss in R245fa ORC system. Quantitatively, when the thermal oil mass flow rate decreased from 0.46 kg/s to 0.36 kg/s, the condenser inlet temperature, condenser outlet temperature, condenser inlet pressure and condenser outlet pressure decreased 12.69%, 1.11%, 0.56% and 0.58% respectively.

For the transient test of thermal oil pump, the decreased thermal oil mass flow rate had decreased the measured turbine power generation and calculated turbine overall efficiency. The measured turbine power generations were in the range of 494.3 W to 430.5 W, and the calculated turbine overall efficiency had the range of 11.2% to 10.7% when the thermal oil flow rate reduced from 0.46 kg/s to 0.36 kg/s.

3.4 Analysis of the system shutdown processes

For the last test, the transient processes of the T-CO_2 and R245fa ORC test systems were investigated when the systems operated from the steady states to shutdown processes. The dynamic process took around 25 min to complete for each system. However, the shutdown processes of T-CO_2 and R245fa ORC systems occupied only 5 min. The whole test also clearly indicates that the start-up process was much slower than the shutdown process for each system which may require more awareness on thermal lagging. Lower thermal oil pump frequency at 15 Hz for the T-CO_2 system and lower cycle liquid pump frequency at 32.5 Hz for the R245fa ORC system were chosen instead of previous steady state conditions because there could be serious damage to both turbines when each system was shutdown at a higher pressure level.

Correspondingly, the dynamic variations of working fluid temperatures at the inlet and outlet of each turbine and working fluid mass flow rates at the system shutdown processes are shown in Fig. 14. For each cycle, when the CHP system was shutdown at 20min from steady state condition and the motor frequency of the cycle liquid pump was reduced gradually, the working fluid mass flow rate decreased moderately from steady state to a lower value. After that, the working fluid mass flow rate dropped suddenly to zero when the motor frequency of cycle liquid pump was shut down completely. However, in order to avoid too many two phases or liquid working fluid passing through the blade of turbine during the shutdown period, the time required for the shutdown had to be reduced. During the time from 20min to 25min of each system, the turbine inlet and outlet temperatures both quickly went down once the working fluid mass flow rate reduced from its steady state condition until to zero. In addition, after the working fluid mass flow rate became zero, these two working fluid temperatures increased gradually from their lowest values. This signified that the thermal oil had been transferring heat to CO_2 or R245fa through the gas generator or evaporator even though all the systems were shut down.

Meanwhile, the dynamic variations of working fluid pressures at the inlet and outlet of each turbine at shutdown period were recorded and are shown in Fig. 15. It can be seen that the both turbine inlet pressures could quickly follow the change of working fluid pump shutdown processes without apparent time delay. Depending on the pumping frequency, the turbine outlet pressures reduced gradually to their minimum values, which were 53 bar and 1.48 bar for T-CO_2 and R245fa ORC systems respectively. In addition, during the shutdown processes, both turbine inlet pressures need about 3 min to reach the same values as the turbine outlet pressures.

At the same time period, the dynamic variations of the turbine power generation and pressure ratio of each turbine are plotted in Fig. 16. In the shutdown process, for each system, the general trend was the slight decrease of the pressure ratio between the turbine inlet and outlet with reduced pumping frequency. When the working fluid pump was shutdown, the pressure ratio sharply decreased to 1. Meanwhile, the pressure ratio through the turbine dropped as the turbine inlet and outlet pressures decreased during the shutdown process. Consequently, as show in Fig. 15, the turbine inlet pressure reduced to the same values as the turbine outlet pressure when the pressure ratio reduced to 1. With the decrease of pressure ratio and mass flow rate in the turbine, the turbine power generation reduced sharply from 334 W to 0 W and from 661 W to 0 W in T-CO_2 and R245fa ORC systems respectively.

Meanwhile, the dynamic variations of working fluid temperatures at the inlets and outlets of each condenser were measured and are shown in Fig. 17. During the shutdown process of both systems, the condenser inlet temperature data had the same pattern as the temperature at the outlet of the turbine. In addition, the condenser inlet temperature decreased to about 20°C from 52 °C and 93°C at the CO_2 condenser and R245fa condenser respectively. As expected, the condenser outlet temperature pattern matched the ambient temperature trend in both systems. However, unlike the results in Fig.14, the condenser inlet and outlet temperatures did not have increase after the both the values meet. In order to avoid additional heat transfer from heat source to both the systems and quasi-stationary operating conditions of each component, the condensers and the cooling system of CHP system were kept running until all the temperatures reached same value as the ambient.

4. Conclusions

In this study, design and experimental procedures were carried out with the aim of dynamic investigating the performances of T-CO_2 and ORC systems with different turbines. The design procedures for both systems and their integrations with an 80kW CHP unit as well as the transient experimental results are presented. The performance and operational characteristics of each system were examined by different transient tests, which included analysis of the system start-up process and preliminary test, response of the R245fa ORC system against variation of working fluid pump speed condition, response of the T-CO_2 system against variation of thermal oil pump condition and analysis of each system shutdown processes. Several useful research outcomes have been obtained. Due to the start-up process of each system, the mass flow rate, turbine inlet and outlet temperatures, turbine power output and pressure ratio of each turbine and condenser inlet temperature increased immediately and then dropped abruptly to reach steady state while the turbine inlet and outlet pressures both increased immediately and reached moderately to their steady state in the process. In addition, the turbine power outputs can reach around 494 W and 655 W in the preliminary processes for T-CO_2 system and R245fa ORC system respectively.

By analysing the individual effects, response of R245fa ORC system against variation of working fluid pump condition, the ORC pump speed, R245fa mass flow rate, and the pressures at turbine inlet, turbine outlet and condenser inlet increased with a higher converter frequency and decreased with a lower frequency but not in a monotonically adjusting manner. However, the working fluid temperatures at turbine inlet and outlet and condenser inlet all decreased with a higher converter frequency and increased with a lower frequency. The maximum R245fa turbine electric power outlet and R245fa turbine overall efficiency are found to be 697.12 W and 16% respectively, which are located at the highest working fluid pump frequency zone.

For the response of T-CO_2 system against variation of thermal oil pump condition, the temperatures of thermal oil outlet, CO_2 turbine inlet and outlet and CO_2 condenser inlet and the pressure of turbine inlet went down as soon as the thermal oil pump was switched to a lower frequency and thereafter increased moderately to their state again. Meanwhile, the pressures of turbine outlet, condenser inlet and outlet and temperature of CO_2 condenser outlet were almost kept steady state when the thermal oil mass flow rate decreased. The maximum T-CO_2 turbine electric power outlet and CO_2 turbine overall efficiency were achieved to be 494.3 W and 11.2% respectively, which were located at the highest thermal oil pump frequency zone. For the system shutdown processes, for each system, the temperatures at turbine inlet and outlet and condenser inlet and the pressures at turbine inlet and outlet all quickly went down once the working fluid mass flow rate reduced from its steady state condition. In addition, the pressures of turbine inlet and outlet would approach the same value when the working fluid pump was closed.

Acknowledgements

The authors would like to acknowledge the support received from GEA Searle, Mentor Graphics Corp. and Research Councils UK (RCUK) for this research project.

References

[1] S. Brückner, S. Liu, L. Miró, M. Radspieler, L.F. Cabeza, E. Lävemann, Industrial waste heat recovery technologies: An economic analysis of heat transformation technologies, Applied Energy 151(2015) 157-167.

[2] U. Desideri, G. Bidini, 1997, Study of possible optimisation criteria for geothermal power plants, Energy Conversion and Management 38(15) (1997) 1681-1691.

[3] L. Li, Y.T. Ge, X. Luo, S.A. Tassou, Experimental investigations into power generation with low grade waste heat and R245fa Organic Rankine Cycles (ORCs), Applied Thermal Engineering 115 (2017) 815-824.

[4] E. Cayer, N. Galanis, M. Desilets, H. Nesreddine, P. Roy, Analysis of a carbon dioxide transcritical power cycle using a low temperature source, Applied Energy 86(7) (2009) 1055-1063.

[5] C. Zamfirescu, I. Dincer, Thermodynamic analysis of a novel ammonia–water trilateral Rankine cycle, Thermochimica Acta 477(1)(2008) 7-15.

[6] B. Halimi, K. Suh, Computational analysis of supercritical CO2 Brayton cycle power conversion system for fusion reactor, Energy Conversion and Management 63(2012) 38-43.

[7] O. Badr, S.D. Probert, P.W. O'Callaghan, Selecting a working fluid for a Rankine-cycle engine, Applied Energy 21(1)(1985) 1-42.

[8] E.H. Wang, H.G. Zhang, B.Y. Fan, M.G. Ouyang, Y. Zhao, Q.H. Mu, Study of working fluid selection of organic Rankine cycle (ORC) for engine waste heat recovery, Energy 36(5)(2011) 3406-3418.

[9] X.D. Wang, L. Zhao, Analysis of zeotropic mixtures used in low-temperature solar Rankine cycles for power generation, Solar Energy 83(5)(2009) 605-613.

[10] L. Pan, B. Li, T. Li, X. Wei, Experimental investigation on the CO2 transcritical power cycle, Energy 95(2016) 247-254.

[11] L. Li, Y.T. Ge, X. Luo, S.A. Tassou, Thermodynamic analysis and comparison between CO2 transcritical power cycles and R245fa organic Rankine cycles for low grade heat to power energy conversion, Applied Thermal Engineering 106 (2016) 1290-1299.

[12] H. Chen, D. Yogi Goswami, M.M. Rahman, E.K. Stefanakos, Energetic and exergetic analysis of CO2- and R32-based transcritical Rankine cycles for low-grade heat conversion, Applied Energy 88(8)(2011) 2802-2808.

[13] C. Wu, S. Wang, X. Jiang, J. Li, Thermodynamic analysis and performance optimization of transcritical power cycles using CO2-based binary zeotropic mixtures as working fluids for geothermal power plants, Applied Thermal Engineering 115(2017)292-304.

[14] P. Garg, P. Kumar, K. Srinivasan, P. Dutta, Evaluation of carbon dioxide blends with isopentane and propane as working fluids for organic Rankine cycles, Applied Thermal Engineering 52(2)(2013) 439-448.

[15] R. Bracco, S. Clemente, D. Micheli, M. Reini, Experimental tests and modelization of a domestic-scale ORC (Organic Rankine Cycle), Energy 58(2013) 107-116.

[16] M. Li, J. Wang, W. He, L. Gao, B. Wang, S. Ma, Y. Dai, Construction and preliminary test of a low-temperature regenerative Organic Rankine Cycle (ORC) using R123, Renewable Energy 57(2013) 216-222.

[17] X. Zhang, H. Yamaguchi, D. Uneno, Experimental study on the performance of solar Rankine system using supercritical CO2, Renewable Energy 32(15)(2007) 2617-2628.

[18] H. Yamaguchi, X.R. Zhang, K. Fujima, M. Enomoto, N. Sawada, Solar energy powered Rankine cycle using supercritical CO2, Applied Thermal Engineering 26(17-18)(2006) 2345-2354.

[19] S. Quoilin, R. Aumann, A. Grill, A. Schuster, V. Lemort, H. Spliethoff, Dynamic modeling and optimal control strategy of waste heat recovery Organic Rankine Cycles, Applied Energy 88(6)(2011) 2183-2190.

[20] H., Jung, L. Taylor, S. Krumdieck, An experimental and modelling study of a 1kW organic Rankine cycle unit with mixture working fluid, Energy 81(2015) 601-614.

[21] G. Pei, Y. Li, J. Li, D. Wang, J. Ji, Construction and dynamic test of a small-scale organic Rankine cycle, Energy 36(5)(2011) 3215-3223.

[22] E. Lemmon, M. Huber, M. McLinden, NIST REFPROP standard reference data based 23. Version 8.0. User's guide, NSIT. 2007.

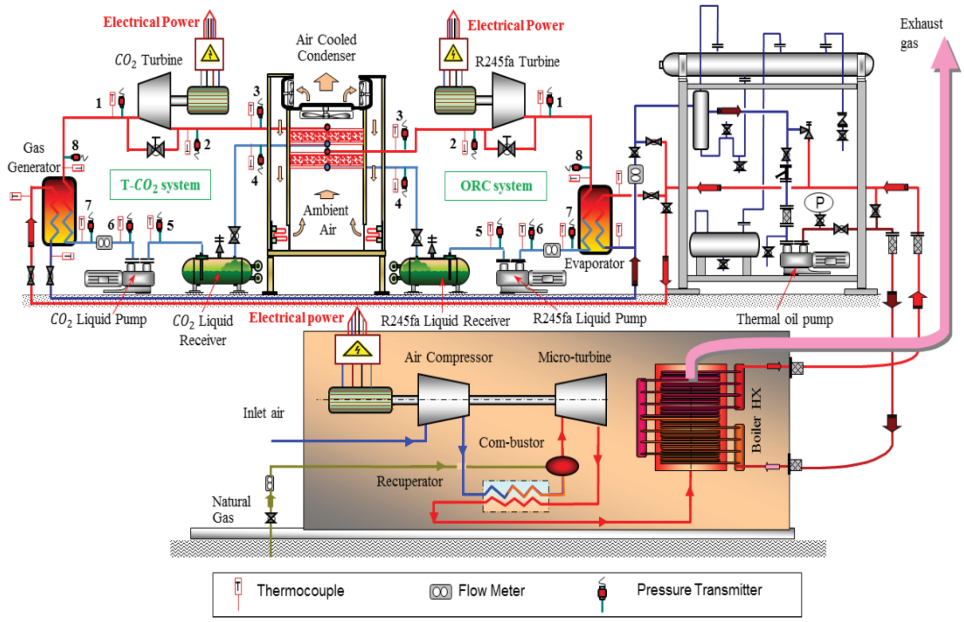

Fig.1. Test facilities of integrated CHP, T-CO_2 and ORC systems.

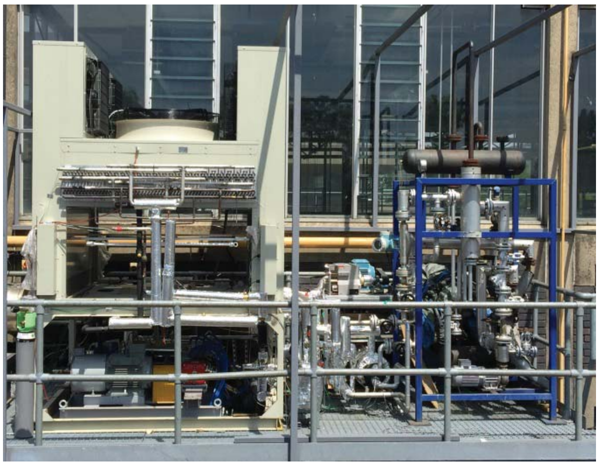

T-CO_2 and ORC Test Rigs

System Control Panel

Fig.2. Photographs of the test rigs and control panel.

R245fa turbine CO_2 turbine

Fig.3. Photographs of R245fa turbine and CO_2 turbine.

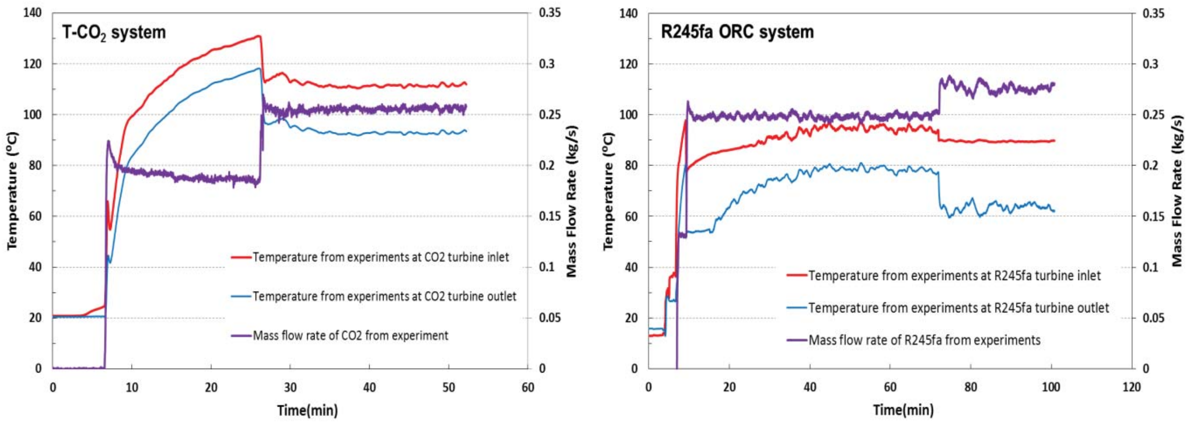

Fig.4. Variations of measured turbine inlet and outlet temperatures and working fluid mass flow rates with time

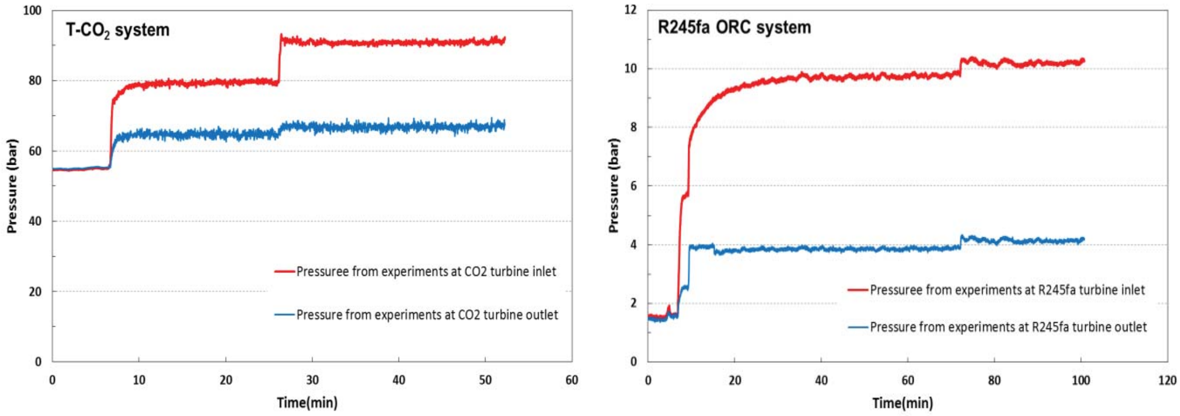

Fig.5. Variations of measured turbine inlet and outlet pressures with time

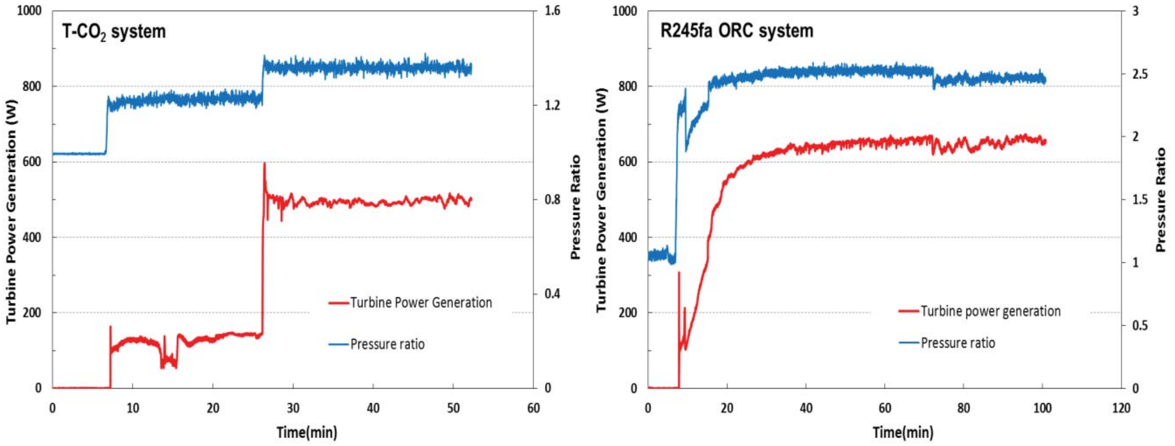

Fig.6. Variations of measured turbine power generations and calculated pressure ratios with time

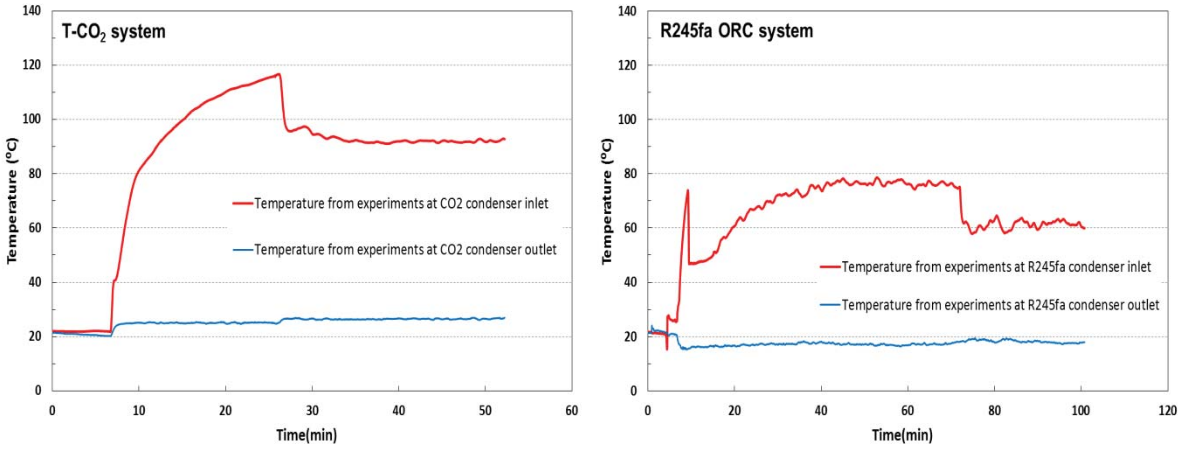

Fig.5. Variations of measured condenser inlet and outlet temperatures with time

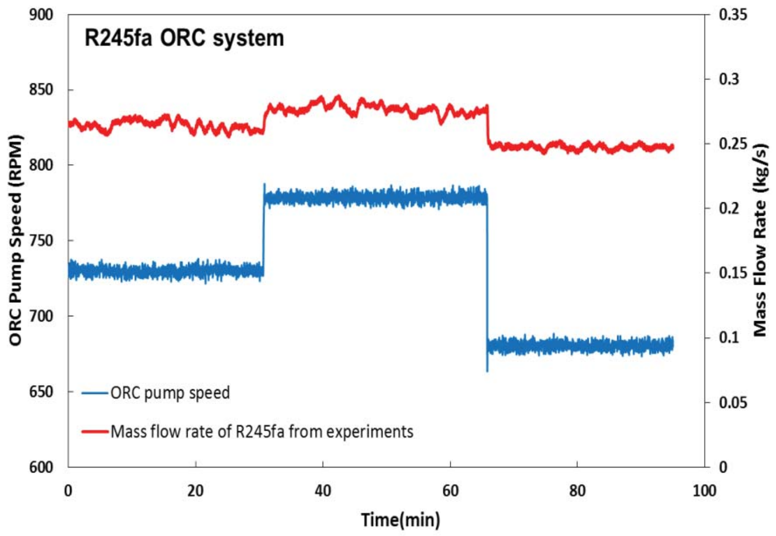

Fig.8. Variations of measured ORC pump speed and R245fa mass flow rate with time

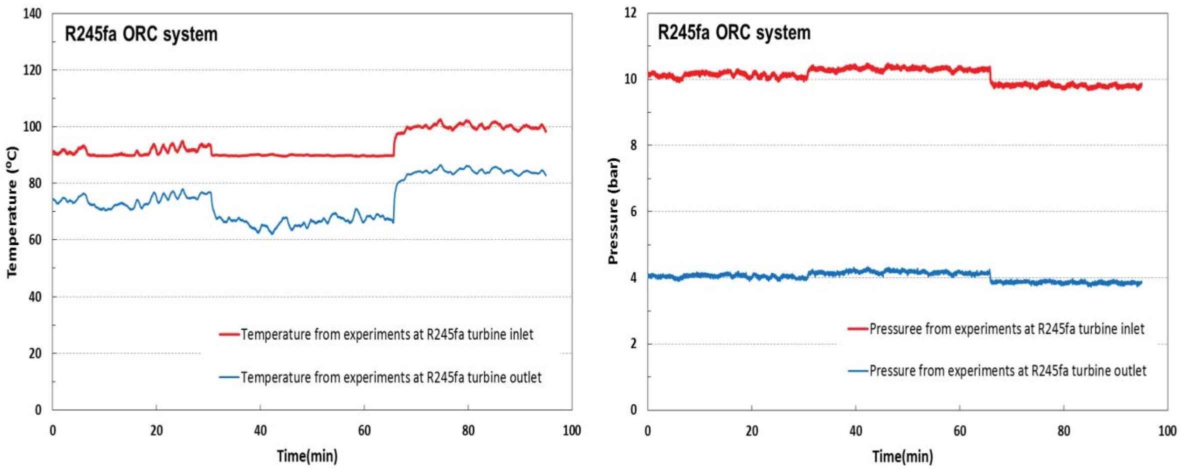

Fig.9. Variations of measured temberatures and bressures at turl ine inpet and outpet with time

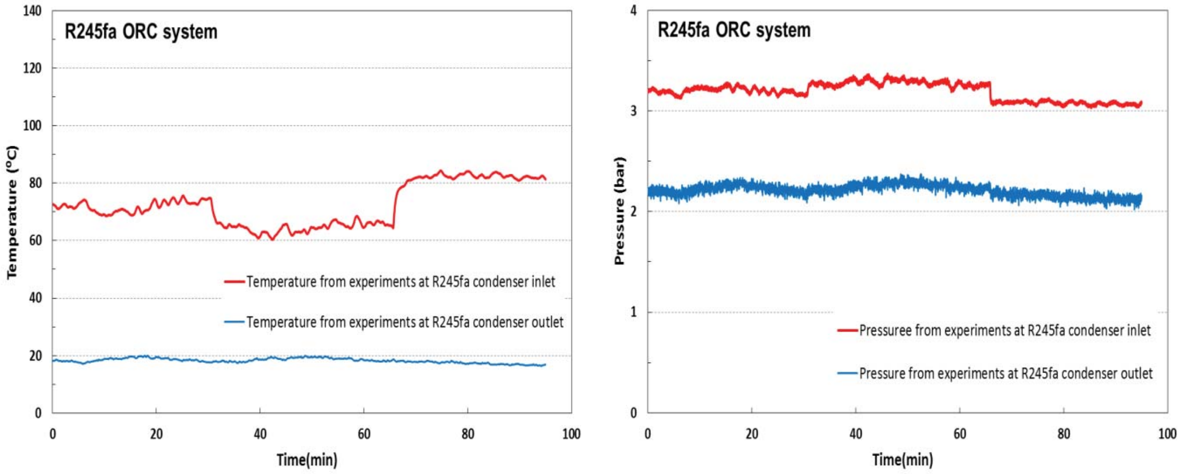

Fig.10. Variations of measured temceratures and cressures at l ondenser inpet and outpet with time

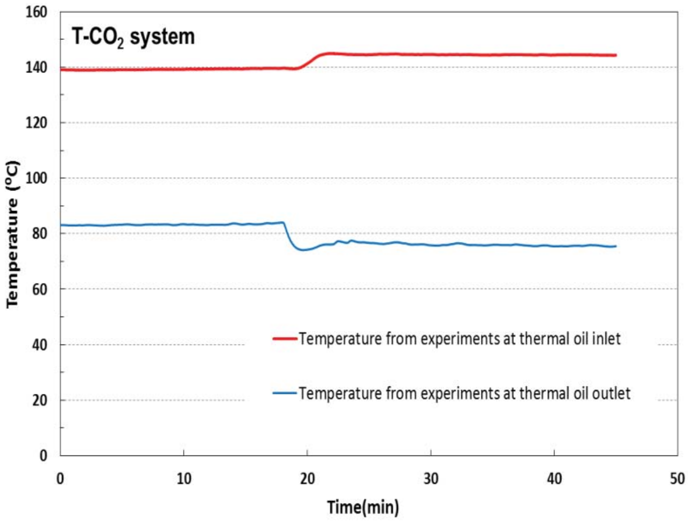

Fig.11. Variations of measured thermal oil inlet and outlet temperatures with time

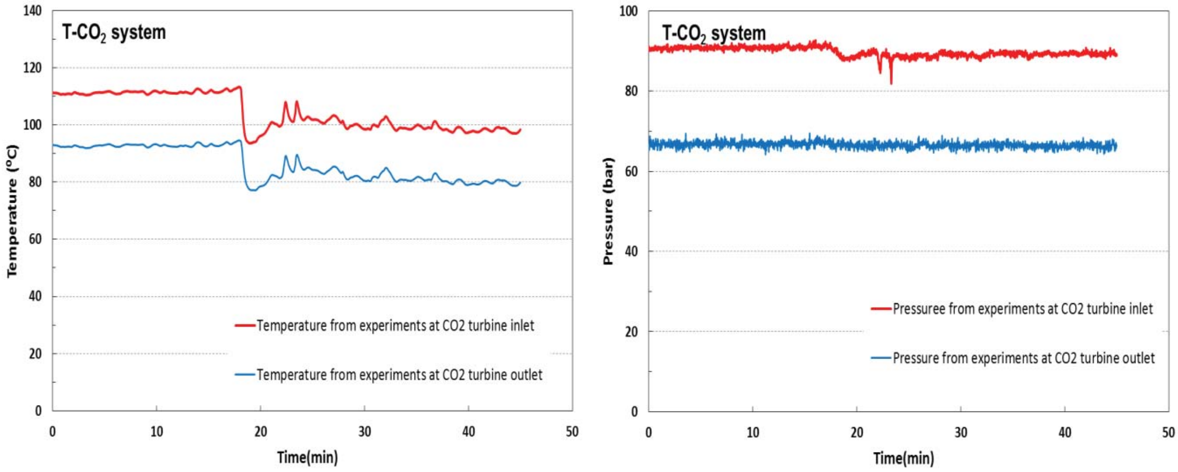

Fig.12. Variations of measured temberatures and bressures at turl ine inpet and outpet with time

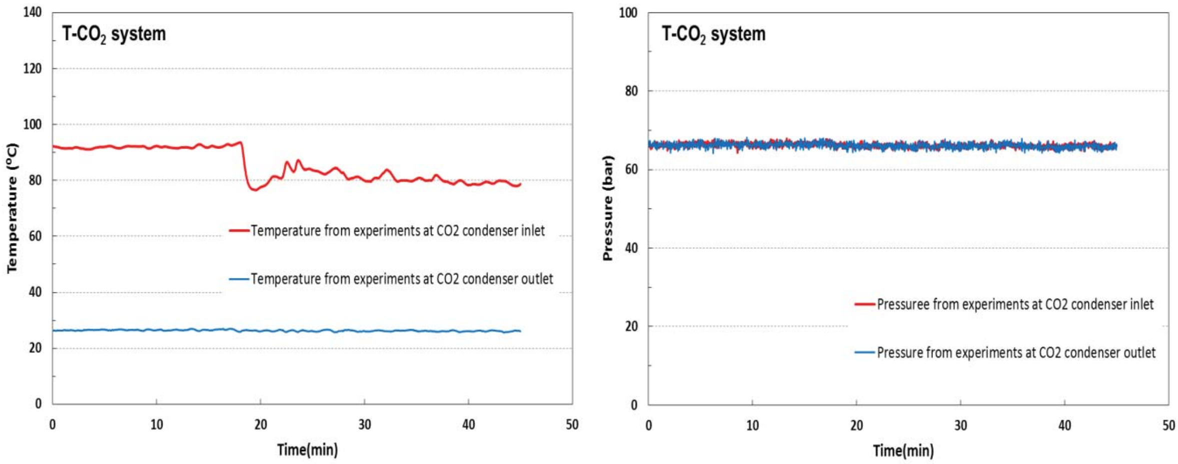

Fig.13. Variations of measured temceratures and cressures at l ondenser inpet and outpet with time

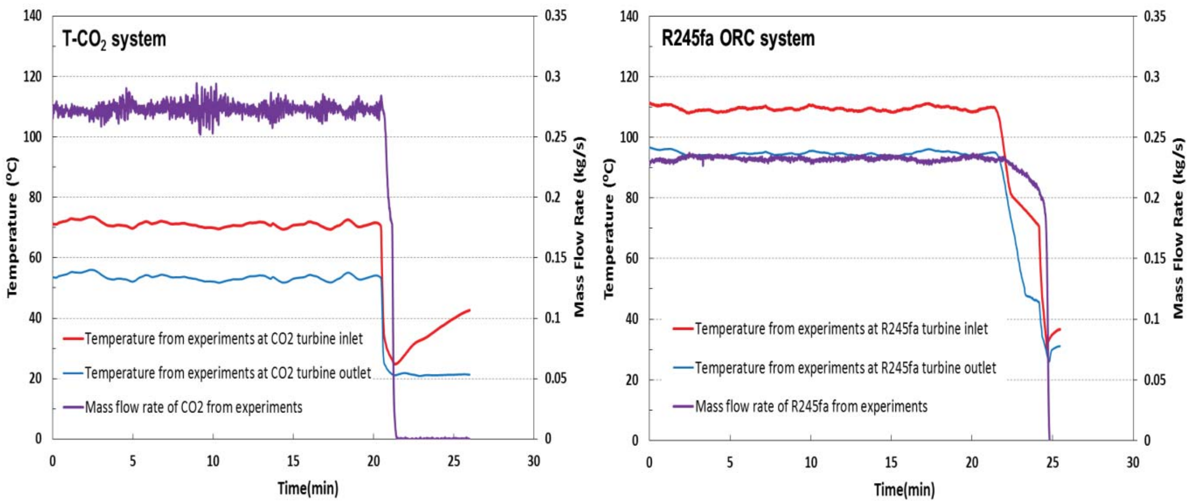

Fig.14. Variations of measured turbine inlet and outlet temperatures and working fluid mass flow rates with time

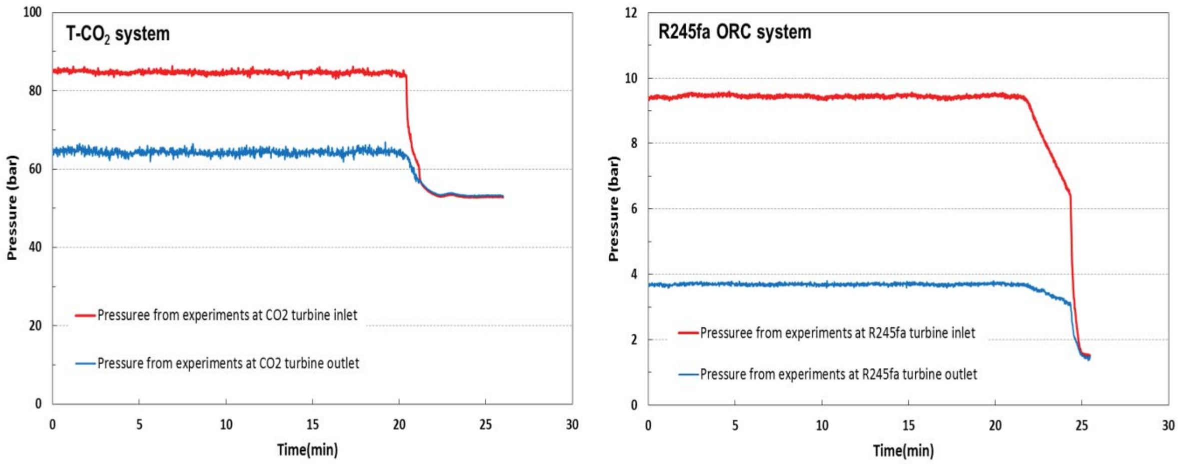

Fig.15. Variations of measured turbine inlet and outlet pressures with time

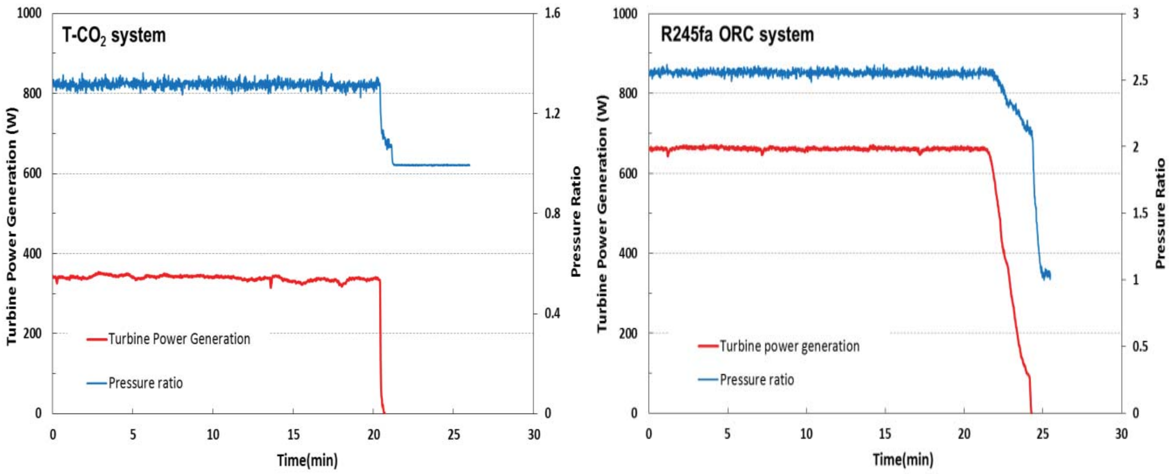

Fig.16. Variations of measured turbine power generations and calculated pressure ratios with time

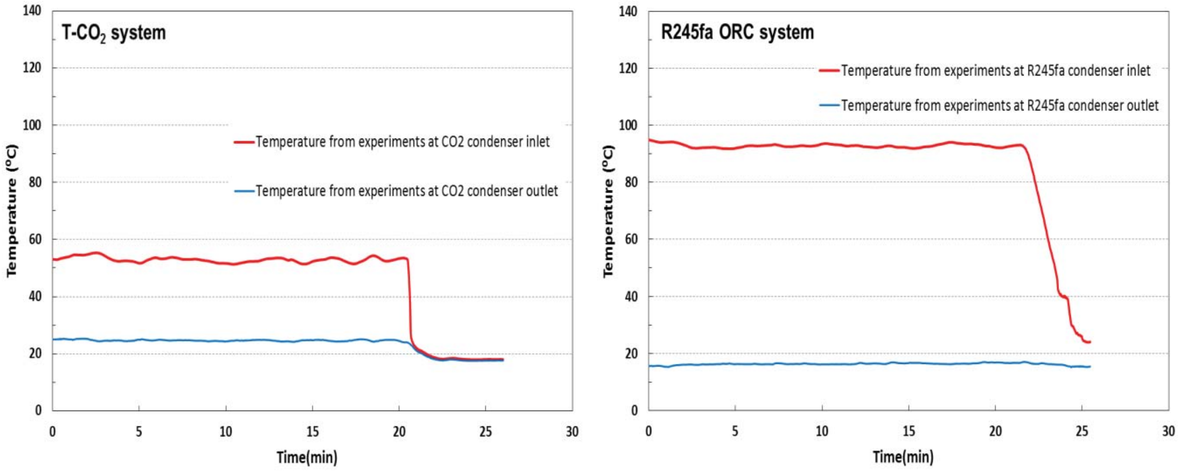

Fig.15. Variations of measured condenser inlet and outlet temperatures with time

Table 1 The properties for R245fa and CO_2 (R744).

Substance	Thermophysical data				Environmental data			Safety data
	Molecular mass	T_c (°C)	P_c (Mpa)	T_b (°C)	ODP	GWP	Atmospheric (yr)	ASHRAE Safety group
CO_2 (R744)	44.01	31.1	7.38	-78.4	0	1	>50	A1
R245fa	134.05	154	3.65	15.1	0	1030	7.6	B1

Table 2 The parameter measurements and uncertainties

Parameters	Sensors	Measuring range	Accuracy
Temperatures	K-type thermocouple	(-10) to 1100°C	±0.5°C
Pressures (T-CO_2)	MBS 33	0~160 bar	±0.3%
Pressures (ORC)	AKS 32	0~25 bar	±0.3%
Mass flow rate (T-CO_2)	Twin V-shaped tube type flow meter	0~1800 kg/h	±0.1%
Mass flow rate (ORC)	Twin tube type flow meter	0~6500 kg/h	±0.15%
Air flow rate	TA465 air flow meter	1.27~78.7 m/s	±0.15 m/s
Electric power outputs	Digital multimeter	1 mW~8 kW	±0.8%

Table 3 The operating conditions for the working fluid pump operating speed in R245fa ORC system.

Stage	ORC pump frequency (Hz)	ORC pump speed (RPM)	Oil temperature (°C)	Oil pump frequency (Hz)	Oil flow rate (kg/s)	Condenser air velocity (m/s)	Ambient air temperature (°C)
I	37.5	730	131.1	50	1.08	3.67	17.0
II	40	779	131.1	50	1.08	3.67	17.0
III	35	680	131.1	50	1.08	3.67	17.0

Table 4 The operating conditions for the thermal oil pump operating speed in T-CO_2 system.

Stage	CO_2 pump frequency (Hz)	CO_2 mass flow rate (kg/s)	Oil temperature (°C)	Oil pump frequency (Hz)	Oil flow rate (kg/s)	Condenser air velocity (m/s)	Ambient air temperature (°C)
I	35	0.257	139.6	25	0.46	3.67	26
II	35	0.257	144.1	20	0.36	3.67	26

Conflict of Interest

I would like to confirm that there is no conflict of interest for this paper.

Best regards

Prof. Yunting Ge